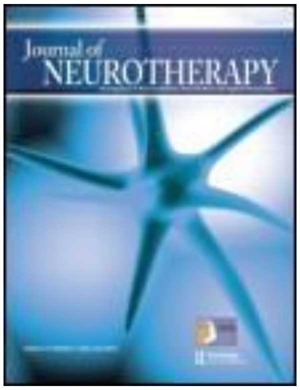

Journal of Neurotherapy: Investigations in Neuromodulation, Neurofeedback and Applied Neuroscience

A Comparative Investigation of Wavelet Families for Analysis of EEG Signals Related to Artists and Nonartists During Visual Perception, Mental Imagery, and Rest

Nasrin Shourie [a] , S. Mohammad P. Firoozabadi [b] & Kambiz Badie [c]

[a] Department of Biomedical Engineering , Islamic Azad University , Tehran , Iran
[b] Faculty of Medical Sciences , Tarbiat Modares University , Tehran , Iran
[c] Research Institute for ICT , Tehran , Iran
Published online: 04 Dec 2013.

To cite this article: Nasrin Shourie , S. Mohammad P. Firoozabadi & Kambiz Badie (2013) A Comparative Investigation of Wavelet Families for Analysis of EEG Signals Related to Artists and Nonartists During Visual Perception, Mental Imagery, and Rest, Journal of Neurotherapy: Investigations in Neuromodulation, Neurofeedback and Applied Neuroscience, 17:4, 248-257, DOI: 10.1080/10874208.2013.847606

To link to this article: http://dx.doi.org/10.1080/10874208.2013.847606

Journal of Neurotherapy, 17:248–257, 2013

ISSN: 1087-4208 print/1530-017X online
DOI: 10.1080/10874208.2013.847606

Routledge
Taylor & Francis Group

A COMPARATIVE INVESTIGATION OF WAVELET FAMILIES FOR ANALYSIS OF EEG SIGNALS RELATED TO ARTISTS AND NONARTISTS DURING VISUAL PERCEPTION, MENTAL IMAGERY, AND REST

Nasrin Shourie[1], S. Mohammad P. Firoozabadi[2], Kambiz Badie[3]

[1]Department of Biomedical Engineering, Islamic Azad University, Tehran, Iran
[2]Faculty of Medical Sciences, Tarbiat Modares University, Tehran, Iran
[3]Research Institute for ICT, Tehran, Iran

Differences between the multichannel EEG signals of artists and nonartists were investigated using wavelet coefficients during visual perception and mental imagery tasks and at rest. The wavelet coefficients were calculated using wavelet functions such as Daubechies (order 1–10), Coiflets (order 1–5), and biorthogonal (order 2.4). Each of the calculated approximation and detail coefficients and their averages, standard deviations, and their energies were separately used for discriminating the two groups. The Davies-Bouldin Index was used for evaluation of the feature space quality. We found that the two groups are discriminable using the wavelet coefficients calculated by all of the studied wavelet functions. It was also observed that level of decomposition does not contribute significantly to discriminability. In addition, we observed no considerable difference between approximation and detail coefficients for discriminating the two groups. It was also found that a distinguishing coefficient may exist among the wavelet coefficients, which can discriminate the two groups despite electrode placement. However, separating the two groups is dependant on channel selection when using the energy, average, and standard deviation of the wavelet coefficients. Finally, the two groups were classified by selected wavelet coefficients and a neural gas classifier. The average classification accuracy was 100% for classification of the two groups in the at-rest condition.

INTRODUCTION

Much research to date has evaluated the differences between EEG signals of experts and nonexperts during and prior to performance of a skill. Previous research has investigated the EEG signals of experts such as artists and sportsmen. These studies found that the patterns of cortical activity of experts and nonexperts are different (Abernethy & Russell, 1987; Bhattacharyaa & Petsche, 2002; Bird, 1987; Collins, Powell, & Davies, 1990; Crews & Landers, 1993; Fink, Graif, & Neubauer, 2009; Hatfield, Landers, & Ray, 1984; Haufler, Spalding, Maria, & Hatfield, 2000; Karkare, Saha, & Bhattacharya, 2009; Panga, Nadalb, Müllerc, Rosenbergd, & Kleine, 2012; Petsche, Lindner, Rappelsberger, & Gruber, 1988; Petsche, Richter, Stein, Etlinger, & Filz, 1993; Radlo, Steinberg, Singer, Barba, & Melinkov, 2002; Salazar et al., 1990; Shourie, Firoozabadi, & Badie, 2011, 2013; Wagner, 1975a, 1975b). Most of the previous research has focused on the power spectrum density of the traditional EEG rhythms, which may not be reliable due to the nonstationary nature of the EEG signals (Collins et al., 1990; Crews & Landers, 1993; Fink et al., 2009; Hatfield et al., 1984; Haufler et al., 2000; Petsche et al., 1988; Petsche et al., 1993; Radlo

Received 23 May 2013; accepted 8 September 2013.
We thank Professor Joydeep Bhattacharya for his valued effort in providing us the EEG data.
Address correspondence to Nasrin Shourie, PhD, Science & Research Branch, Islamic Azad University, Department of Biomedical Engineering, Hesarak, Pounak, Tehran, Iran. E-mail: shourie.n@srbiau.ac.ir

et al., 2002; Salazar et al.,1990; Shourie et al., 2013; Wagner, 1975a, 1975b). Hence, time-frequency features are highly reliable for EEG signal analysis.

Wavelet transform can provide time-frequency features. Therefore, many researchers use the wavelet transform for biological signal analysis (Adeli, Zhou, & Dadmehr, 2003; Gandhi, Panigrahi, & Anand, 2011; Gandhi, Panigrahi, Bhatia, & Anand, 2010; Ghosh-Dastidar, Adeli, & Dadmehr, 2007; Horrell, El-Baz, Baruth, Tasman, & Sokhadze, 2010; Hu, Wang, & Ren, 2005; Jahankhani, Kodogiannis, & Revett, 2006; Sparto, Parnianpour, Barria, & Jagadeesh, 2000). For example, Adeli et al. (2003) used discrete Daubechies and harmonic wavelets to study epileptic EEG signals. They found that the transient features of EEG signals are accurately determined and localized in both time and frequency contexts using wavelet transform. Jahankhani et al. (2006) recorded EEG signals from healthy volunteers while at rest and from epileptic patients during a seizure. They decomposed the EEG signals into details D1–D4 and one final approximation, A4, using a discrete wavelet transform. Features such as minimum, maximum, mean, and standard deviation of the wavelet coefficients at different subbands were calculated. Finally, the two groups were classified using MLP and RBF classifiers (Jahankhani et al., 2006). Ghosh-Dastidar et al. (2007) applied a wavelet transform to decompose EEG signals into delta, theta, alpha, beta, and gamma frequency subbands. Horrell et al. (2010) used a wavelet transform for extracting the gamma rhythm from EEG signals. Gandhi et al. (2010) investigated epileptic and seizure-free EEG signals of the same person using wavelet transform. They decomposed both of the EEG data sets into approximation and detail coefficients up to the sixth-level using a db4 wavelet function. Therefore, they discriminated the epileptic and the seizure-free EEG signals using energy values of the approximation coefficients and a probabilistic neural network classifier. In another study, different wavelet functions were assessed for EEG decomposition. It was found that Coiflets1 is the most appropriate function for classification of the EEG signals (Gandhi et al., 2011). Sparto et al. (2000) considered fatigue of two trunk muscles (Erector spine and Latisimus dorsi) using a wavelet transform. They observed that fatigue increment yields a significant elevation in the 13–22 Hz wavelet component of EMG signals. Hu et al. (2005) employed a wavelet packet for feature extraction from EMG signals. They classified two kinds of limb actions using the wavelet packet energy at different frequency subbands.

In this article, we investigated differences between EEG signals of artists and nonartists. A review of research suggests employment of wavelet transform for artistic expertise analysis. Previous research has studied differences between EEG signals of artists and nonartists. For instance, Bhattacharya and Petsche (2002) found that phase synchrony is significantly higher in artists compared to non-artists in the high frequency bands during visual perception. Karkare et al. (2009) classified artists and nonartists by scaling exponents and an artificial neural network-based classifier. Their average classification accuracy was 81.6%. Other researchers have investigated differences between EEG signals of artists and nonartists in scaling exponents, too. They observed that scaling exponents discriminate the two groups when they are at rest. However, discriminability in scaling exponents between the two groups decreases during the performance of similar cognitive tasks (Shourie et al., 2011). In addition, it has been observed that artistic expertise is related to reduced ERP responses to visual stimuli (Panga et al., 2012). However, there is no broad research that has investigated differences between the two groups in terms of wavelet coefficients.

This study explores how wavelet transform may help to differentiate EEG signals of artists and nonartists. It was not clear which wavelet function is appropriate when considering artistic expertise and which wavelet dependant feature is proper for discriminating the two groups. In addition, differences between the two groups may be only observed in some of the channels; however, the best channels for discriminating the two groups via wavelet coefficients were not known.

This research sought to find the answers to the aforementioned issues. Therefore, the EEG signals were decomposed using various wavelet functions such Daubechies (order 1–10), Coiflets (order 1–5), and biorthogonal (order 2.4). Each of the calculated wavelet coefficients was used for discriminating the two groups. The feature space quality was evaluated using the Davies-Bouldin Index (DBI). We determined which wavelet functions are appropriate for artistic expertise analysis. The suitable level of decomposition was determined. The wavelet coefficients of each of the channels were considered separately. It was also determined which channels are appropriate for discriminating the two groups. Energy, average, and standard deviation of the calculated wavelet coefficients were used for discriminating the two groups, too. Finally, it was ascertained whether wavelet transform is an appropriate tool for artistic expertise analysis.

METHODS

Data Set

This study utilized the EEG signals that were obtained in a study by Karkare et al. (2009). The participants in their research consisted of 20 women who were equally divided into two groups—artists and nonartists. Artists graduated from the Viennese Academy of Fine Arts with an MA degree, and nonartists had no specific interest or training in visual art. The average ages of the two groups were 44.3 and 37.5 years old, respectively. The EEG signals were recorded at 19 electrode sites while the subjects performed four tasks of visual perception, four tasks of mental imagery and at rest. The electrodes were placed according to the International 10–20 System (Fp1, Fp2, F7, F3, Fz, F4, F8, T3, C3, Cz, C4, T4, T5, P3, Pz, P4, T6, O1, and O2). The sampling frequency was 128 Hz. In the visual perception condition, participants looked at a painting presented onto a white wall for 2 min. In the mental imagery task, they mentally imagined the painting just shown for 2 min. In the at-rest condition, they looked at a white wall for 2 min (Karkare et al., 2009).

DISCRETE WAVELET TRANSFORM

A wavelet is a smooth waveform that has limited length and an average value of zero. Wavelet transform multi-resolution analysis was first proposed by Mallet in 1989. This transform is a linear operation that decomposes a signal into different frequency subbands with appropriate localization in both time and frequency domains. Wavelet transform is implemented using a pair of FIR filters called quadrature mirror filters (QMFs). One of these FIR filters is a high-pass filter that separates high-frequency components of an input signal. The other is a low-pass filter that extracts the low-frequency components of the signal. The outputs of QMFs are de-sampled with a factor of two. The output of the low-pass filter is fed to another pair of QMFs. Consequently, the input signal is decomposed into different frequency subbands. The outputs of the high-pass and the low-pass filters are called detail and approximation coefficients, respectively (Mallat, 1989; Gandhi et al., 2011). The wavelet decomposition tree up to the fourth level is shown in Figure 1.

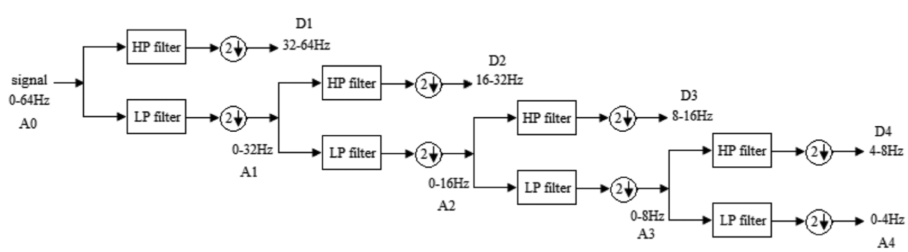

FIGURE 1. Wavelet decomposition tree up to the fourth level.

In this research, the obtained wavelet coefficients were used for discriminating the two groups. In addition, some parameters of the approximation and the detail coefficients were used for separating the two groups. For this purpose, the average, energy, and standard deviation values were selected as parameters of the obtained wavelet coefficients.

DAVIES-BOULDIN INDEX

The DBI was used for cluster validity. The DBI is designed based on scattering matrices. For calculation of this index, the distance between clusters should be obtained, and then the worst discriminability should be found for each of the clusters. Finally, the worst discriminabilities for all of the clusters should be averaged. The DBI calculation procedure can be expressed as follows:

$$DB = \frac{1}{c}\sum_{i=1}^{c} R_i \tag{1}$$

where c is the number of the clusters and R_{ij} is the similarity between cluster i and j.

$$R_i = \max_{j \in c, j \neq i} \left\{ \frac{s_i + s_j}{D_{ij}} \right\} \tag{2}$$

where s_i and s_j are the scattering matrices of *ith* and *jth* clusters. D_{ij} represents the distance between *ith* and *jth* clusters.

$$s_i = \left[\frac{1}{J_i} \sum\nolimits_{j=1}^{J_i} \left\| X_j - Z_i \right\|^p \right]^{1/p} \qquad X_j \in \mathit{cluster}\ i \tag{3}$$

DBI measures discriminability between clusters. A lower DBI value indicates more discriminability between the clusters. A higher DBI value shows more similarity between the clusters (Davies & Bouldin, 1979). The range of classification accuracy can be predicted by the DBI value. In this approach, if the DBI value is lower than 2.5, one can expect classification accuracy is more than 60%. If the DBI value is lower than 1, then the classification accuracy can be more than 90%.

NEURAL GAS CLASSIFIER

Neural Gas is a competitive network in that it has no certain topology. The number of its neurons is constant during a learning procedure. The neurons of the network are adapted according to their distance to training data. After training, the neurons cover the space of the training data. For classification of an unknown input, its distances to all of the neurons should be calculated. The label of the closest neuron to the unknown input determines its label (Martinetz & Schulten, 1991).

In this article, the obtained features were divided into two groups: training data (80%) and test data (20%). Therefore, the neural gas network was trained by the training data. Then the trained network was tested by the test data.

RESULTS

DBI Values Calculation

The EEG signals were decomposed by the wavelet functions such as Daubechies (order 1–10), Coiflets (order 1–5), and biorthogonal (order 2.4) up to the first level. The EEG signals were related to the two groups in the at-rest condition. The level of the decomposition was fixed at the first level to evaluate the role of the various wavelet functions for separating the two groups. The calculated approximation and detail coefficients were analyzed separately. DBI values were obtained for each of the calculated wavelet coefficients. The wavelet coefficient with the lowest value in the DBI was determined for each of the tasks and channels separately. The obtained results are shown in Tables 1 and 2. The best channels are highlighted for each of the considered wavelet functions.

Accordingly, we found that the reported DBI values were low for all of the wavelet functions and channels. This means that the two groups are discriminable by wavelet coefficients in the at-rest condition. In this case, no

TABLE 1. The Lowest Davies-Bouldin Index Values Related to the Approximation Coefficients of Each of the Channels for Discriminating the Two Groups in the At-Rest Condition

CH	db1	db2	db3	db4	db5	db6	db7	db8	db9	db10	Coif1	Coif2	Coif3	Coif4	Coif5	bior2.2
Fp1	0.6662	0.6478	0.6795	0.7421	0.8204	0.9117	0.9820	0.7935	0.6847	0.6415	0.9171	0.9376	0.9463	0.9498	0.9508	0.9593
Fp2	0.9612	0.9978	0.9833	0.9764	0.9835	1.0121	1.0619	1.0772	1.0285	0.9766	0.9698	0.9898	0.9971	1.0012	1.0042	1.0285
F7	0.9778	0.9944	1.0387	0.9629	0.8608	0.8078	0.8041	0.8557	0.9752	1.0404	0.9645	0.9353	0.9229	0.9154	0.9101	0.9083
F3	0.9050	0.8926	0.8953	0.8921	0.8550	0.8363	0.8486	0.8779	0.9024	0.8804	0.8866	0.8881	0.8898	0.8907	0.8912	0.8858
Fz	0.9218	0.9248	0.9342	0.9415	0.9136	0.9052	0.9238	0.9461	0.9129	0.8946	0.9474	0.9515	0.9532	0.9547	0.9562	0.9300
F4	1.0583	1.0615	1.0766	1.1058	1.1270	1.0822	1.0471	1.0222	1.0076	1.0035	1.0588	1.0601	1.0626	1.0646	1.0661	1.0554
F8	0.7210	0.7486	0.8173	0.8960	0.9169	0.8946	0.8876	0.8905	0.8597	0.8033	0.8759	0.8735	0.8726	0.8724	0.8726	0.8456
T3	0.8632	0.8274	0.8320	0.7999	0.8087	0.8762	0.9615	0.9750	0.9551	0.9330	0.9538	0.9587	0.9651	0.9689	0.9708	0.9780
C3	0.9816	0.9963	0.9701	0.9239	0.8579	0.8047	0.7776	0.7857	0.8279	0.8978	0.8086	0.8039	0.8027	0.8014	0.8003	0.7853
Cz	0.9668	1.0123	0.9491	0.8648	0.8071	0.7773	0.7757	0.8023	0.8584	0.9494	0.7900	0.7825	0.7796	0.7780	0.7771	0.7562
C4	1.1449	1.1409	1.1417	1.1434	1.1478	1.1413	1.1154	1.1028	1.1069	1.1296	1.1376	1.1388	1.1382	1.1372	1.1363	1.1817
T4	0.9054	0.8440	0.7836	0.7795	0.8307	0.9333	1.0477	0.9503	0.9118	0.9166	0.9727	0.9730	0.9729	0.9730	0.9732	0.9703
T5	0.7528	0.8167	0.8122	0.7829	0.7585	0.7797	0.8536	0.8580	0.8584	0.8834	0.7978	0.8052	0.8070	0.8076	0.8077	0.7895
P3	0.8263	0.8122	0.7840	0.8051	0.8595	0.9103	0.8963	0.8782	0.8622	0.8513	0.8935	0.9051	0.9091	0.9111	0.9121	0.8643
Pz	1.0870	1.0819	1.0344	1.0134	1.0164	1.0382	1.0604	1.0485	1.0549	1.0413	1.0072	1.0099	1.0121	1.0135	1.0145	1.0055
P4	1.0824	1.0828	1.0867	1.0905	1.0867	1.0487	0.9095	0.8713	0.9075	0.9972	0.9619	0.9498	0.9496	0.9511	0.9527	0.9448
T6	1.0052	1.0437	1.0533	0.9635	0.9180	0.8919	0.8770	0.8973	0.9538	1.0494	0.9251	0.9080	0.9033	0.9022	0.9025	0.8317
O1	0.8311	0.8132	0.8206	0.8197	0.8101	0.8408	0.8826	0.8848	0.9049	0.9255	0.8823	0.8891	0.8906	0.8910	0.8909	0.9037
O2	1.0146	0.9771	0.9536	0.9468	0.9517	0.9635	0.9717	0.9912	1.0024	1.0121	1.0056	1.0134	1.0186	1.0218	1.0239	0.9743

Note. The approximation coefficients were calculated by the various wavelet functions.

considerable changes in reported DBI values were observed related to the various wavelet functions. Also, no noticeable changes were found in the DBI values of the best coefficients for all of the channels. In addition, no considerable differences were observed between the approximation and the detail coefficients for discriminating the two groups.

Second, the EEG signals were decomposed using db5 up to the sixth level. The wavelet type was fixed and the level of decomposition was varied to observe the role of decomposition level for separating the two groups. The two groups were compared during visual perception, mental imagery, and at-rest tasks using the approximation and the detail coefficients, separately. Hence, DBI values were calculated for the obtained wavelet coefficients of each of the channels and levels among the four trials. The best wavelet

TABLE 2. The Lowest Davies-Bouldin Index Values Related to the Detail Coefficients of Each of the Channels Discriminating the Two Groups in the At-Rest Condition

CH	db1	db2	db3	db4	db5	db6	db7	db8	db9	db10	Coif1	Coif2	Coif3	Coif4	Coif5	bior2.2
Fp1	1.0108	1.0493	1.0474	0.9795	0.9286	0.9844	0.9075	0.9483	0.9451	1.0073	0.8784	1.1091	1.0679	1.0851	0.9751	0.9493
Fp2	1.0805	0.9962	1.0316	1.0745	1.0259	1.0784	0.9315	0.9108	0.9182	0.9244	0.9897	1.1268	0.9002	0.8569	1.0005	1.0177
F7	1.0536	1.0763	1.0838	1.0647	1.0730	1.0129	1.1003	1.0104	0.8453	0.9645	1.0560	0.9285	0.9543	0.9920	0.6688	0.8519
F3	0.7288	0.7549	0.6924	0.6714	0.6923	0.7561	0.9074	0.9622	0.9954	0.9482	0.6718	0.7885	0.9677	1.0481	0.8049	0.9317
Fz	0.7834	0.8528	0.7903	0.7368	0.7372	0.7398	0.8780	1.0096	0.9745	0.9257	0.8182	0.9233	0.8960	1.1706	1.0660	1.0234
F4	1.0233	1.0303	1.0655	1.1088	0.9705	1.0353	0.9862	0.9669	0.8301	0.9370	1.1333	1.0690	1.0755	0.9238	0.9823	0.9486
F8	0.8834	0.9423	0.9305	0.9125	0.8990	0.8973	1.0499	0.9309	1.0401	0.9860	0.8654	0.9397	0.9907	1.0041	0.8487	0.9903
T3	0.8593	0.9137	0.9277	0.9635	0.9766	0.8116	0.8200	0.9219	0.8733	0.7847	0.8720	1.0653	0.9845	0.9180	0.9704	0.8805
C3	1.0428	0.8652	0.8954	0.9403	0.9487	0.9908	0.9194	0.9127	1.0136	0.7681	0.9470	0.9485	1.0925	1.0671	0.8728	0.8373
Cz	1.0648	1.0208	1.0411	0.9975	1.0169	1.1041	0.9848	1.0294	0.9582	0.8429	0.9515	0.8126	0.9672	1.0494	1.0297	0.9201
C4	0.8785	0.9251	0.9336	0.9159	0.9747	0.7583	0.9408	0.8786	0.6653	0.8449	0.9579	0.9951	1.0011	0.9719	0.8825	0.9750
T4	1.0593	1.0237	1.0507	1.0759	0.9990	1.0104	0.8719	1.0045	0.9858	0.9846	0.9562	1.0048	1.0264	0.9351	1.1817	1.0602
T5	0.9362	0.9027	0.8820	0.8674	0.8685	0.9440	0.9732	0.7715	0.9256	0.8992	0.9999	0.8744	0.9626	0.6570	0.7421	0.7374
P3	0.7086	0.9842	0.9522	0.9428	0.8776	0.7434	0.7676	0.8047	0.9639	0.8471	0.8296	0.7649	0.6935	0.9452	0.9530	0.8391
Pz	0.9866	0.7369	0.7382	0.7779	0.9446	0.8962	0.9752	0.8380	0.9923	0.9048	0.9344	0.8784	0.9253	0.9897	0.9346	0.9570
P4	0.8291	0.8722	0.8743	0.9062	1.0351	0.7822	0.9664	0.8876	0.7494	0.8685	0.8568	0.9228	0.8969	0.8691	0.7769	0.9915
T6	1.0513	0.9764	0.9892	1.0452	1.0013	1.0291	0.9263	0.7681	0.7688	0.8806	0.9142	0.8605	0.8364	0.9591	0.7301	0.8832
O1	0.9519	1.0789	1.1070	1.0632	1.1030	0.9077	0.8651	0.9249	0.9951	1.0334	1.1129	1.1322	1.0489	0.9137	0.9426	0.8873
O2	0.8895	0.7063	0.7106	0.7144	0.7243	0.9876	0.8885	0.9250	1.0367	0.8547	0.6655	0.8083	0.9448	0.8398	0.8259	0.8936

Note. The detail coefficients were calculated by the various wavelet functions.

TABLE 3. The Indices of the Approximation Coefficients With the Lowest Davies-Bouldin Index Values for Each of the Channels and Decomposition Level for Discriminating the Two Groups During the Visual Perception Task

	Level1		Level2		Level3		Lelve4		Level5		Level6	
CH	Index	DB	Index	DB	Index	DB	Index	DB	Index	DB	Index	DB
Fp1	1241	2.2770	624	2.1138	316	2.4092	189	2.7576	97	2.5374	40	3.7520
Fp2	1456	2.3179	732	2.4102	874	2.4949	441	2.7226	224	2.6897	57	4.3529
F7	2818	2.0061	1413	2.3014	710	2.2368	396	2.2444	196	2.7571	95	3.4736
F3	3391	2.4605	1699	2.4006	537	2.7173	187	3.1515	219	3.0529	52	3.8116
Fz	2499	2.3205	1253	2.4621	316	2.4542	319	2.5311	97	3.2185	37	4.0316
F4	1241	2.2898	691	2.6559	316	2.8104	319	2.9129	224	2.9458	100	3.3378
F8	1254	2.3583	1447	2.8009	160	2.8466	368	2.6604	188	2.8790	98	4.3851
T3	2691	2.2947	1827	2.5015	785	2.8539	396	2.4834	202	2.9341	115	3.9558
C3	1241	2.3351	1827	2.4658	316	2.5899	383	2.8426	195	2.5596	101	3.1913
Cz	1241	2.6463	624	2.6918	316	2.5078	187	3.1446	195	2.8118	100	2.8456
C4	1241	2.1696	624	2.3925	367	2.7927	187	2.9632	195	2.5772	100	3.0264
T4	2865	2.3936	1451	2.8355	729	2.8296	368	2.8991	188	2.8249	39	2.7160
T5	2882	2.4740	1013	2.3472	183	2.4412	181	2.7086	36	2.8009	100	2.3852
P3	1240	2.3866	624	2.3503	316	2.7792	440	3.1109	195	2.6378	100	2.2405
Pz	1240	2.4160	624	2.4829	873	2.8094	187	2.9683	195	2.4608	100	2.4895
P4	832	2.3056	1013	2.5148	510	2.5115	105	2.9233	195	2.3201	100	2.9089
T6	3094	1.9605	234	2.3809	257	2.4928	378	2.7066	195	2.5997	39	2.7550
O1	2998	2.0344	233	2.1300	120	2.3492	64	2.5524	36	2.4956	100	2.7154
O2	247	2.2413	358	2.5483	120	2.3238	64	2.6738	59	2.4777	100	2.4516

Note. The Davies-Bouldin Index value related to each of the selected coefficients is noted. The wavelet coefficients were calculated by db5.

coefficients were determined for each of the channels and levels. Tables 3 through 6 show the obtained results.

In conclusion, we found that the two groups are distinguishable during visual perception, mental imagery, and at-rest conditions

TABLE 4. The Indices of the Detail Coefficients With the Lowest Davies-Bouldin Index Values for Each of the Channels and Decomposition Level for Discriminating the Two Groups During the Visual Perception Task

	Level1		Level2		Level3		Lelve4		Level5		Level6	
CH	Index	DB	Index	DB	Index	DB	Index	DB	Index	DB	Index	DB
Fp1	286	1.9087	131	2.8693	126	2.3616	364	2.6994	158	2.8205	102	2.6946
Fp2	1574	2.6739	1037	2.5138	477	3.0234	197	2.1949	170	3.3936	42	2.6625
F7	2673	2.3365	58	1.9733	50	2.0368	356	2.5090	178	3.2773	102	2.2314
F3	1191	2.3521	1255	2.0933	173	2.3367	41	2.7609	202	3.4054	110	2.8914
Fz	735	2.2895	8	2.1204	173	2.5799	288	2.8956	10	3.8063	102	3.2901
F4	1286	2.5788	344	2.1943	552	2.7047	288	2.9663	10	3.4426	102	3.0505
F8	2772	2.3052	209	2.5845	276	2.6385	364	2.3656	79	2.9095	96	2.5863
T3	1153	2.5463	642	2.2240	908	2.2741	365	2.7828	82	2.8691	66	3.0617
C3	1152	2.1213	8	2.2503	535	2.6755	353	2.7974	82	3.1892	110	3.8317
Cz	1075	2.6395	806	2.1559	530	2.8078	288	3.0084	233	3.0930	27	3.4682
C4	1286	2.3563	845	2.4539	84	2.7204	13	2.9492	53	2.9664	49	3.5404
T4	2352	2.1760	1782	2.3183	577	2.2554	410	3.1316	53	2.8364	96	2.7481
T5	500	1.8693	215	2.3760	721	2.2414	371	2.5743	82	2.4592	40	3.4981
P3	1152	1.9809	819	2.7046	721	2.1715	115	2.6657	82	3.3507	30	2.8716
Pz	1056	2.2951	604	2.6053	322	2.4437	16	2.6882	160	2.9692	30	2.9350
P4	2539	2.3371	524	2.1561	322	2.2433	16	2.7161	53	2.8877	30	2.2252
T6	2496	2.1746	652	2.0829	6	2.6734	390	2.2976	53	3.0388	30	2.5305
O1	1946	2.1923	215	2.3906	721	2.3176	378	2.6015	221	3.0690	85	3.2975
O2	1567	2.0673	71	2.4861	322	2.5962	378	2.3446	177	3.0356	30	2.3487

Note. The Davies-Bouldin Index value related to each of the selected coefficients is noted. The wavelet coefficients were calculated by db5.

TABLE 5. The Lowest Davies-Bouldin Index Values Related to the Approximation and detail Coefficients Calculated by db5 for Each of the Channels and Various Decomposition Levels for Discriminating the Two Groups During the Mental Imagery Task

	Approximation						Detail coefficients					
CH	Level1	Level2	Level3	Level4	Level5	Level6	Level1	Level2	Level3	Level4	Level5	Level6
Fp1	2.1997	2.3262	2.4614	2.8841	2.8676	2.6501	2.5122	2.5373	2.7204	2.6153	3.1597	2.9984
Fp2	2.2842	2.2544	2.4995	2.4213	2.2371	3.0722	2.6184	2.5294	2.4274	2.7642	2.5870	2.7111
F7	2.3883	2.4759	2.5803	2.5507	2.8695	3.0790	2.1857	1.9358	2.6478	2.5786	2.8965	2.8787
F3	2.2819	2.3914	1.9941	2.8307	3.0689	3.2982	2.3458	2.4300	2.7809	2.4688	2.4864	3.1846
Fz	2.2604	2.6455	2.4476	3.1325	2.9280	3.2493	2.1137	2.3778	2.7125	2.2644	3.0492	2.9087
F4	2.4253	2.4117	2.5990	3.0112	2.3970	3.2415	2.3270	2.3514	2.5046	2.1940	2.9401	3.0493
F8	2.3557	2.5624	2.6959	2.9308	2.4688	2.8465	2.2541	2.6315	2.8816	2.5968	2.7864	2.9809
T3	2.0263	2.1138	1.8358	2.5575	2.7438	2.5350	2.3296	2.5296	2.1704	2.8178	3.6271	3.2014
C3	1.9775	2.0196	2.1697	3.0880	3.0165	3.6612	2.1260	2.6135	2.6405	2.9445	2.7962	3.2104
Cz	2.0345	2.4594	2.5506	2.4907	3.0139	3.1625	2.0971	2.1929	2.5656	2.8699	2.5565	3.5355
C4	2.3176	2.6721	2.8214	2.6110	3.0747	3.0574	2.2048	2.5058	2.1650	2.3331	2.7633	3.0755
T4	2.2057	2.5288	2.5260	3.0436	2.4191	2.7257	2.2873	2.4941	2.1076	2.1546	2.8574	3.4259
T5	1.9881	2.2342	2.0716	2.6138	2.7344	3.6414	2.0765	2.4351	2.3427	2.5550	2.5318	3.1884
P3	2.4176	2.5195	2.6076	2.3944	2.8694	4.1596	2.3393	2.3890	2.6150	2.9317	2.6703	2.5995
Pz	2.3547	2.4702	2.4627	2.6147	2.8479	3.2202	2.1437	2.1542	2.5835	2.7834	2.7056	2.7601
P4	1.9308	2.0330	2.3437	2.3241	2.4982	2.9568	2.0715	2.4911	2.2569	2.6160	2.9589	2.7882
T6	1.8330	1.7464	2.3098	2.4946	2.7159	3.0718	2.1414	2.6030	2.5975	2.6616	2.5859	3.1546
O1	1.9544	2.5938	2.4246	2.6388	3.1635	3.7782	2.7031	2.1889	2.7529	2.4233	2.3409	3.4626
O2	2.3259	2.2725	2.3874	2.7817	3.5396	3.9542	2.1550	2.6630	2.5141	2.6851	2.6604	3.5129

using the approximation and detail coefficients calculated by db5. No noticeable differences were observed between the different channels. The reported DBI values were lower in the at-rest condition compared to the visual perception and mental imagery tasks. Therefore, it is expected that the average classification accuracy of the two groups at rest must be higher. It was also found that an increase in decomposition level was not so significant. However, the best results were often observed in levels of decomposition lower than 4.

Finally, the energy, average, and standard deviation of the approximation and the detail

TABLE 6. The Lowest Davies-Bouldin Index Values Related to the Approximation and detail Coefficients Calculated by db5 for Each of the Channels and Various Decomposition Levels for Discriminating the Two Groups in the At-Rest Condition

	Approximation						Detail coefficients					
CH	Level1	Level2	Level3	Level4	Level5	Level6	Level1	Level2	Level3	Level4	Level5	Level6
Fp1	0.8204	0.8992	1.1779	1.2926	1.3045	1.8465	1.1091	1.0368	1.0835	1.2424	1.3593	1.3667
Fp2	0.9835	0.9140	1.1077	1.4360	1.5856	1.4427	1.1268	1.1001	1.0546	1.0877	1.2617	1.1959
F7	0.8608	1.1648	1.3401	1.2182	1.3308	1.5157	0.9285	0.9653	0.9722	1.3965	1.2358	1.2102
F3	0.8550	0.8173	1.3367	1.5253	1.4896	1.3911	0.7885	0.9536	0.9533	1.3452	1.4948	1.3576
Fz	0.9136	0.9550	1.2385	1.5182	1.4037	1.3445	0.9233	0.8540	1.2770	1.0599	1.6991	1.2004
F4	1.1270	1.1050	1.1257	1.3788	1.4304	1.0795	1.0690	1.0030	1.0624	1.0221	1.4431	1.3185
F8	0.9169	0.9472	1.1854	1.2166	1.2586	1.3515	0.9397	0.9959	1.0561	1.0878	1.0294	1.2157
T3	0.8087	0.8124	1.0739	1.1808	1.3442	1.1141	1.0653	1.0466	1.1186	1.3244	1.2759	1.4015
C3	0.8579	0.9509	1.0879	1.2016	1.2646	1.7069	0.9485	0.9607	1.1195	1.4366	1.2673	1.4656
Cz	0.8071	0.9554	1.0533	1.1053	1.3488	1.6191	0.8126	0.8079	1.1817	1.2773	1.3585	1.2760
C4	1.1478	1.1065	1.1797	1.3569	1.2243	1.3072	0.9951	1.0091	1.1029	0.9257	1.2391	1.2312
T4	0.8307	1.0510	1.0772	1.0501	1.4218	1.4218	1.0048	1.1526	1.0181	0.9783	0.9964	1.1114
T5	0.7585	0.9946	1.0642	1.1381	1.4033	1.1052	0.8744	1.0351	1.0452	1.3738	0.9457	1.4918
P3	0.8595	0.7776	0.9932	1.2617	1.0801	1.2689	0.7649	0.8376	0.8521	1.1308	0.9001	1.3102
Pz	1.0164	1.0625	1.0489	1.1064	1.0856	1.3207	0.8784	1.1371	1.2000	1.1119	0.9587	1.5919
P4	1.0867	1.0814	1.0295	1.1659	1.2617	1.6704	0.9228	1.0219	1.0838	1.2650	0.9447	1.4142
T6	0.9180	0.9462	1.1040	1.1504	1.2168	1.5023	0.8605	0.9687	1.1921	1.2484	1.0056	1.1375
O1	0.8101	1.0075	0.8458	1.1442	1.2800	1.4591	1.1322	0.7395	0.7882	1.1111	1.1290	1.5051
O2	0.9517	1.0598	0.9599	0.9870	1.4476	1.2153	0.8083	0.8743	1.2496	1.4329	1.1633	1.4354

Table 7. The Davies-Bouldin Index Values for the Average, the Standard Deviation, and the Energy of the Approximation and Detail Coefficients Related to the Two Groups in the At-Rest Condition for Each of the Channels

	Approximation						Detail coefficients					
	Level 1			Level 2			Level 1			Level 2		
CH	Mean	SD	Energy	Mean	SD	Energy	Mean	SD	Energy	Level 4	Level 5	Level 6
Fp1	3.1702	19.875	40.985	3.8743	9.6799	27.492	23.533	4.4234	2.9543	4.0598	4.2880	2.9622
Fp2	3.9914	16.918	60.879	3.3760	10.346	16.654	15.480	3.5611	2.8537	131.95	4.5091	3.3999
F7	2.4913	3.1386	2.7780	2.5733	3.4397	3.0058	3.5519	3.3357	3.0447	7.2186	2.5632	2.4595
F3	4.2532	16.998	10.859	4.9411	40.768	21.575	3.9690	3.7019	3.0334	5.7424	3.6010	3.0528
Fz	5.7798	17.668	244.68	5.6917	12.639	32.163	28.571	8.9999	6.5411	8.8485	6.9950	5.1041
F4	7.0172	10.328	13.373	6.1922	7.6614	8.4754	7.1368	5.6980	4.5635	55.716	7.8598	5.5883
F8	2.1188	137.54	14.775	2.2418	4746.7	16.629	3.1773	105.02	20.611	2.7642	15.519	8.2829
T3	13.366	36.114	6.3464	13.070	6.8436	7.5767	4.4340	25.075	4.4412	394.44	5.2843	4.5765
C3	21.984	10.744	43.803	13.338	10.874	47.374	13.145	3.9757	3.8264	4.7003	15.220	39.253
Cz	62.020	28.235	16.769	35.939	21.808	19.936	24.519	10.223	14.283	16.434	17.414	8.0410
C4	8.0604	8.4691	11.924	6.5091	7.7730	10.506	7.6169	11.354	9.7217	63.342	134.02	48.086
T4	2.3694	19.265	14.280	2.2897	11.502	11.671	4.8259	13.095	28.436	4.6254	12.295	69.301
T5	72.920	4.4673	4.2435	23.072	4.7365	4.4154	2.4200	3.6024	3.5737	8.8570	4.2782	4.0786
P3	4.5649	6.7406	6.9144	5.2465	7.0670	7.0784	2.4471	2.7581	2.7968	5.3744	6.8409	8.0077
Pz	8.5638	9.0752	9.8126	12.719	8.8482	9.2779	14.544	4.5655	4.5645	21.2702	38.091	92.935
P4	216.51	4.5124	4.0804	26.120	4.5355	4.0767	7.4550	4.6180	4.3355	11.7143	7.5643	6.8391
T6	29.588	4.0322	3.8361	17.416	3.7901	3.5954	1.3831	15.748	16.6155	15.8983	14.7727	13.508
O1	2.5984	2.2831	2.2078	3.1493	2.5550	2.4432	2.7986	2.2805	2.3392	10.6160	1.8823	1.9207
O2	2.3749	3.3123	2.9281	3.4751	3.5791	3.1390	2.0773	4.2477	4.0264	10.3372	2.4897	2.2227

coefficients calculated by db5 were investigated. The wavelet coefficients were related to the two groups in the at-rest condition. The obtained results are shown in Table 7. The best channels are highlighted for each of the features.

As shown in Table 7, it was observed that the two groups are distinguishable using the energy, standard deviation, and average of the wavelet coefficients. But, in this approach, the separation of the two groups is dependant on channel selection.

Classification of the EEG Signals

In this research, some of the channels were randomly selected for classification of the two groups. The wavelet coefficient with the lowest DBI value was determined for each of the selected channels. The two groups were classified by each of the determined wavelet coefficients and a neural gas classifier. The obtained average classification accuracies are shown in Table 8.

TABLE 8. The Average Classification Accuracies Related to the Two Groups During the Visual Perception, the Mental Imagery, and the At-Rest Conditions for Some of the Channels Using the Selected Approximation (App) and Detail (Det) Wavelet Coefficients

CH	Wavelet type	Coeff type	Index	Task	Average classification accuracy%
Fp1	Db2	App	2987	Rest	100
Cz	Bior2.4	App	1249	Rest	100
T5	Db3	Det	1665	Rest	91.66
O2	Db6	Det	3060	Rest	91.66
F7	Db3	App	2819	Visual Perception	66
F7	Coif2	App	2822	Visual Perception	62.5
C4	Db3	Det	2109	Visual Perception	75
F8	Coif2	Det	2773	Visual Perception	72.91
T6	Db10	App	2955	Mental Imagery	62.5
O1	Coif1	App	1979	Mental Imagery	66.5
T4	Db6	Det	2478	Mental Imagery	62.5
C4	Coif2	Det	3308	Mental Imagery	75

Accordingly, it was observed that the average classification accuracy is highest (100%) in the two groups in the at-rest condition. The obtained classification accuracies show that wavelet transform is an appropriate tool for artistic expertise analysis.

DISCUSSION

In this article, differences between the EEG signals of artists and nonartists were analyzed using wavelet coefficients. It was found that the type of wavelet function and electrode placement is not so significant in this regard. This is because a distinguishing coefficient may exist among the wavelet coefficients that can discriminate the two groups despite the type of wavelet function and the placement of the electrode. It was also observed that level of signal decomposition is not significant for separating the two groups. We also observed that was no considerable difference between the approximation and the detail coefficients for discriminating the two groups in all of the decomposition levels, which means that both low- and high-frequency components can be employed for separating the two groups for each of the decomposition levels. Taking into account the aforementioned points, it becomes clear that differences between artists and nonartists can be observed in all of the traditional EEG signal rhythms.

It was also determined that the DBI values are lower in the at-rest condition. Therefore, it is expected that the average classification accuracy for the two groups must be higher in the at-rest condition. The obtained classification results confirmed this issue. This indicates that discriminability in wavelet coefficients between the groups decreases during the visual perception and the mental imagery tasks. This result is similar to the results reported by Shourie et al. (2011) declaring that discriminability in scaling exponents between artists and nonartists is higher in the at-rest condition compared to the performance of similar cognitive tasks.

REFERENCES

Abernethy, B., & Russell, D. G. (1987). Expert-novice differences in an applied selective attention task. *Sport Psychology*, *9*, 326–345.

Adeli, H., Zhou, Z., & Dadmehr, N. (2003). Analysis of EEG records in an epileptic patient using wavelet transform. *Journal of Neuroscience Methods*, *123*, 69–87.

Bhattacharya, J., & Petsche, H. (2002). Shadows of artistry: Cortical synchrony during perception and imagery of visual art. *Cognitive Brain Research*, *13*, 179–186.

Bird, E. I. (1987). Psycho-physiological processes during rifle shooting. *International Journal of Sports Psychology*, *18*, 9–18.

Collins, D., Powell, G., & Davies, I. (1990). An electroencephalographic study of hemispheric processing patterns during karate performance. *Journal of Sport and Exercise Psychology*, *12*, 223–234.

Crews, D. J., & Landers, D. M. (1993). Electroencephalographic measures of attentional patterns prior to the golf putt. *Medicine and Science in Sports and Exercise*, *25*, 116–126.

Davies, D. L., & Bouldin, D. W. (1979). A cluster separation measure. *IEEE Transactions on Pattern Analysis and Machine Intelligence*, *1*, 224–227.

Fink, A., Graif, B., & Neubauer, A. C. (2009). Brain correlates underlying creative thinking: EEG alpha activity in professional vs. novice dancers. *NeuroImage*, *46*, 854–862.

Gandhi, T., Panigrahi, B. K., & Anand, S. (2011). A comparative study of wavelet families for EEG signal classification. *Neurocomputing*, *74*, 3051–3057.

Gandhi, T., Panigrahi, B. K., Bhatia, M., & Anand, S. (2010). Expert model for detection of epileptic activity in EEG signature. *Expert Systems with Applications*, *37*, 3513–3520.

Ghosh-Dastidar, S., Adeli, H., & Dadmehr, N. (2007). Mixed-band wavelet-chaos-neural network methodology for epilepsy and epileptic seizure detection. *IEEE Transactions on Biomedical Engineering*, *54*, 1545–1551.

Hatfield, B. D., Landers, D. M., & Ray, W. J. (1984). Cognitive processes during self paced motor performance: An electroencephalographic profile of skilled marksmen. *Journal of Sport Psychology*, *6*, 42–59.

Haufler, A. J., Spalding, T. W., Maria, D. L. S., & Hatfield, B. D. (2000). Neuro-cognitive activity during a self-paced visuospatial task: Comparative EEG profiles in marksmen and novice shooters. *Biological Psychology*, *53*, 131–160.

Horrell, T., El-Baz, A., Baruth, J., Tasman, A., & Sokhadze, G. (2010). Neurofeedback effects on evoked and induced EEG gamma band reactivity to drug-related cues in cocaine addiction. *Journal of Neurotherapy*, *14*, 195–216.

Hu, X., Wang, Z., & Ren, X. (2005). Classification of surface EMG signal using relative wavelet packet energy. *Computer Methods and Programs in Biomedicine*, *79*, 189–195.

Jahankhani, P., Kodogiannis, V., & Revett, K. (2006, October). *EEG signal classification using wavelet feature extraction and neural networks*. Paper presented at the IEEE John Vincent Atanasoff 2006 International Symposium on Modern Computing, Sofia, Bulgaria.

Karkare, S., Saha, G., & Bhattacharya, J. (2009). Investigating long-range correlation properties in EEG during complex cognitive tasks. *Chaos, Solitons and Fractals*, *42*, 2067–2073.

Mallat, S. G. (1989). A theory for multiresolution signal decomposition: The wavelet representation. *IEEE Transactions on Pattern Analysis and Machine Intelligence*, *11*, 674–693.

Martinetz, T. M., & Schulten, K. J. (1991). A neural gas network learns topologies. *Artificial Neural Networks*, *1*, 397–402.

Panga, C. Y., Nadalb, M., Müllerc, J. S., Rosenbergd, R., & Kleine, C. (2012). Electrophysiological correlates of looking at paintings and its association with art expertise. *Biological Psychology*, *93*, 246–254.

Petsche, H., Lindner, K., Rappelsberger, P., & Gruber, G. (1988). The EEG: An adequate method to concretize brain processes elicited by music. *Music Perception*, *6*, 133–159.

Petsche, H., Richter, P., Stein, A. V., Etlinger, S. C., & Filz, O. (1993). EEG coherence and musical thinking. *Music Perception*, *11*, 117–151.

Radlo, S. J., Steinberg, G. M., Singer, R. M., Barba, D. A., & Melinkov, A. (2002). The influence of an attentional focus strategy on alpha brain wave activity, heart rate, and dart throwing performance. *International Journal of Sport Psychology*, *33*, 205–217.

Salazar, W., Landers, D. M., Petruzzello, S. J., Myungwoo, H., Crews, D. J., & Kubitz, K. A. (1990). Hemispheric asymmetry, cardiac response, and performance in elite archers. *Research Quarterly for Exercise and Sport*, *61*, 351–359.

Shourie, N., Firoozabadi, S. M. P., & Badie, K. (2011, December). *Information evaluation and classification of scaling exponents of EEG signals corresponding to visual perception, mental imagery & mental rest for artists and non-artists*. Paper presented at the 18th Iranian Conference of Biomedical Engineering, Tehran, Iran.

Shourie, N., Firoozabadi, S. M. P., & Badie, K. (2013). Investigation of EEG alpha rhythm of artists and nonartists during visual perception, mental imagery, and rest. *Journal of Neurotherapy*, *17*, 166–177. doi:10.1080/10874208.2013.813180.

Sparto, P. J., Parnianpour, M., Barria, E. A., & Jagadeesh, J. M. (2000). Wavelet and short-time Fourier transform analysis of electromyography for detection of back muscle fatigue. *IEEE Transactions in Rehabilitation Engineering*, *8*, 433–436.

Wagner, M. J. (1975a). Brainwaves and biofeedback: A brief history—Implications for music research. *Journal of Music Therapy*, *12*, 46–58.

Wagner, M. J. (1975b). Effect of music and biofeedback on alpha brainwave rhythms and attentiveness of musicians and nonmusicians. *Journal of Research in Music Education*, *23*, 3–13.